Temporal Aspects of Rolling Sounds: A Smooth Ball Approaching the Edge of a Plate

C. N. J. Stoelinga, D. J. Hermes, A. Hirschberg, A. J. M. Houtsma
Eindhoven University of Technology, P.O. Box 513, 5600 MB Eindhoven, The Netherlands

Summary
We measured the sounds of smooth metal balls rolling over medium density fiberboard (MDF) plates. In the spectrograms of these sounds we observed gradually varying ripples. These ripples were more closely spaced for the sound generated in the middle of the plate than for the sound generated closer to the edge. Furthermore, the spacing for lower frequencies was somewhat closer than for higher frequencies. It is shown that this pattern arises from the interference between the sound directly generated at the point of contact between ball and plate, and the sound reflected at the edge of the plate. This effect was added to synthesized rolling sounds which resulted in a more natural sound. A discussion is presented concerning the perceptual relevance of this pattern.

PACS no. 43.40.Dx 43.66.Mk 43.20.GP

1. Introduction

This paper is concerned with a spectro-temporal pattern in the spectogram of the sound of a ball rolling over a plate. This study is done in the wider context of a study into the human capabilities of extracting physical and geometric object properties, such as size and shape, from the sounds these objects generate when impacted by other objects. Various authors (e.g., [1, 2, 3]) have shown these capabilities. Until now, the used metal objects with simple geometric forms, and the sound was induced by simple impacts. The acoustical analysis of these systems, as given in these papers, is relatively straight forward; the impact sounds are modelled as a sum of modal frequencies with exponentially decaying envelopes. This was further developed into algorithms to synthesize more complicated impact sounds such as the sounds of balls or pebbles rolling in metal vessels and other hollow metal objects [4]. The results were informally compared with recorded sounds of such systems.

The system we studied consisted of a ball rolling over a wooden plate. Due to strong damping and the absence of clear modal frequencies, the method by Van den Doel *et. al.* could not be applied. Houben *et. al.* [5] demonstrated for a wooden ball rolling over such a wooden plate, that human listeners are capable of distinguishing small from large and slowly from rapidly rolling balls on the basis of their rolling sounds. By signal analysis techniques they then manipulated the spectral and temporal properties of these sounds and could derive from perception experiments with these manipulated sounds that both temporal and spectral properties played a role in the successful

judgement made by the listener. They additionally showed that quasi-periodic amplitude modulation, produced by the not perfectly spherical shape of the wooden balls, when audible, played a dominant role in the judgements by the listeners. For the rest, Houben *et. al.* could not directly link the spectral and temporal signal properties on which the listeners based their judgements with the physical properties of the system that determined these spectral and temporal properties. An obstacle to this was the lack of an acoustic model of the rolling-ball system.

We believe that an appropriate understanding of the acoustic properties of the system is necessary, if we want to understand the temporal and the spectral information in the sound signal that the human listeners use in making judgements about the physical properties of the system, such as the size, material, or velocity of the ball rolling over the plate.

Other studies on rolling sounds [6, 7, 8] focus on the road and railway noise produced by cars and trains. The primary interest of these studies is noise reduction and, hence, they mainly focus on the distribution of acoustic energy over the spectrum. Hardly any attention is paid to temporal and more complicated properties of the noise. Moreover, the physical systems are essentially different from a system consisting of a ball rolling over a plate. For instance, it will be shown that the presence of edges is very important in modelling the acoustics of the ball-plate system.

This study is focused on a spectro-temporal pattern in the spectogram of the rolling sounds of a smooth ball approaching the edge of a wooden plate. The origin of this pattern will be shown to lie in the reflections at the edge of the plate. This effect is first studied by means of cross-correlation techniques, first on unprocessed accelerometer signals, and then on band-pass filtered ver-

sions of these signals. This is used to determine the wave velocity for a range of frequencies. This is of significance since the waves predominantly consist if bending weaves which obey the fourth order dispersive wave equation. For these waves the propagation velocity is frequency dependent, which will appear to be important and this effect will be considered in more detail. A simulation model will be proposed, which is based on signal analyses of recorded sounds. In this model, the mentioned spectro-temporal effects of a ball rolling towards the edge of a plate is included on the basis of a simplified physical analyses. The perceptual relevance of this pattern will be presented.

2. Measurement setup

The vibrations of the plate induced by the rolling ball were recorded using the setup shown in Figure 1. The balls were made of stainless steel and had diameters of either 35 or 55 mm. The plates, 49 cm wide and 122 cm long, consisted of MDF, wood fibers compressed and glued together. Their thickness was 6, 12 or 18 mm. The results used as illustration in the figures of this paper were obtained with the thickest plate.

The setup rested on a table from which it was isolated by a 25 mm thick layer of soft foam. This insulation layer was necessary to avoid vibrations of the table. The effect of the plate's support on our results has been checked by carrying out some measurements on a plate supported by four small soft balloons filled with air. While a reduction in damping of low frequencies is observed the relevant spectro-temporal effects discussed further were not altered. This indicates that the 18 mm thick plate can be considered as "free". Especially for the 6 mm plate, however, the extra damping caused by the foam was very prominent. A possible consequence of this extra damping is a complex wave velocity [9, p173].

In order to give the balls a well defined velocity along the centre line of the plate, they were rolled from a slide onto the plate. The height of the slide was 25 cm. The balls were released from various heights on the slide to vary their velocity. In order to measure the velocity of the ball, its course interrupted the beams of six independent light-gates, placed at intervals of 20 cm. The measurements showed that, during one run, the ball's velocity was constant within a few percent. The range of velocities we used in the experiment was varied from 0.6 to 1.5 m/s.

The slide was separated from the plate by a narrow slit, about 0.5 mm in width, to avoid the transmission of vibrations. The slide had a smooth bend near its end to transform the vertical velocity of the balls into a horizontal one. At the other side of the plate, the ball was left free to roll off.

This experimental setup was chosen in order to prevent bouncing or amplitude modulation by less perfectly round balls. Furthermore, relatively heavy, polished metal balls were used, which resulted in a smooth and stationary rolling sound. In this way, the spectro-temporal pattern could best express itself and was not obscured by bounc-
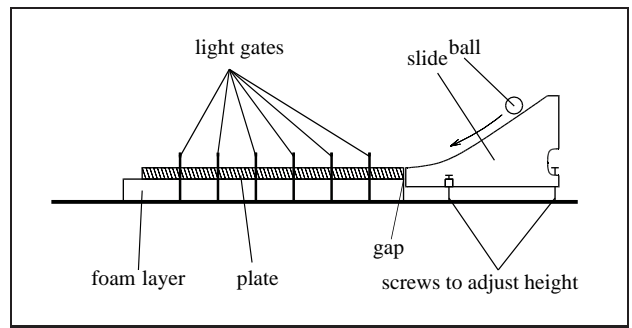

Figure 1. Side-view of the experimental setup: the plate supported by a foam layer is placed on a table. The slide is separated from the plate by a narrow gap. Light-gates are used to measure the velocity of the ball.

ing ticks or other amplitude fluctuations. In fact, the sound generated in this manner does not sound very much like rolling. When the ball is gently slid over the plate, while preventing it from rolling, a similar sound is generated. Hence, the analyses presented here is equally valid for balls sliding softly over the plate.

3. Acoustical analysis

An important variable in the rolling-ball system is the surface roughness of the plate. Surface irregularities of the ball will be ignored, since the ball was made of stainless steel and polished. As long as the velocity of the ball is low, the ball will continuously keep contact with the plate. Due to the surface irregularities it will then move up and down and the corresponding reaction force will excite the plate continuously. When the velocity of the ball gets higher, it may occasionally lose contact with the plate, causing light impacts when it comes down again. Very rough irregularities may also induce such bouncing-like rolling behaviour at lower speeds. The smooth plates we used did not cause such a bouncing.

Even though the ball is in continuous contact with the plate, the interaction is of a non-linear nature. The implications of these non-linear effects have not been fully investigated, but it is assumed that the ball induces a force with band-pass characteristics onto the plate. The plate surface will not contain very low frequencies, since it was polished. Spatial irregularities that are very close together do not move the ball very much either, because it simply rolls over them. Due to these two effects the force that the ball exerts on the plate will have a band-pass character. The frequency range of this band-pass filter scales with the velocity of the rolling ball.

Hence, the spatial-frequency characteristics of the plate roughness and the velocity of the ball determine the bandwidth of the frequencies by which the plate will be excited. In the system we used, this bandwidth was rather broad. An example of an estimated spectrum is shown in Figure 2. It was calculated by averaging the spectra of several successive windowed segments of the signal. This averaging was done to reduce the variance of the spectrum.
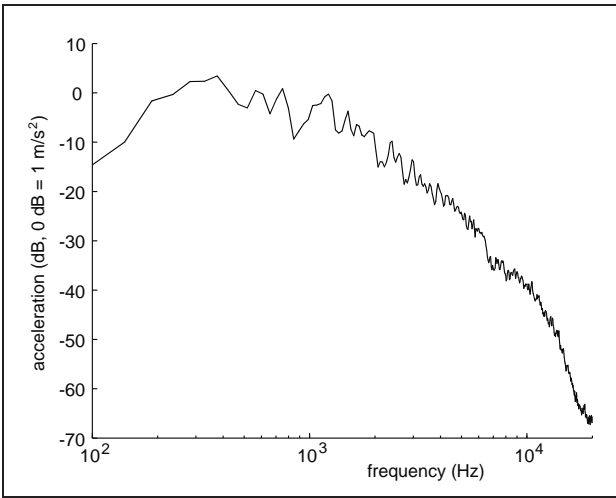
Figure 2. Average spectrum of a ball rolled over the plate.
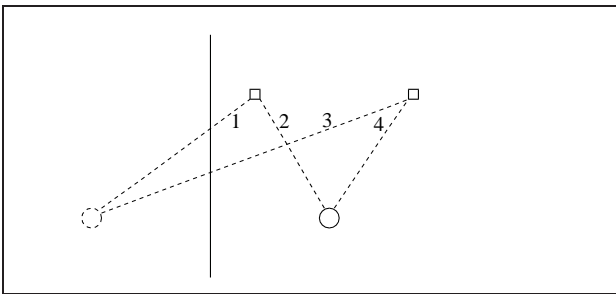

Figure 3. Travelling paths from the ball (marked with a solid circle) to the accelerometer (marked with a square) with a single boundary, resulting in a mirror image of the ball (marked with a dashed circle) and four different paths from the source and its mirror to the accelerometers.

This method results in what is known as Welch averaged periodograms [10].

From the absence of clear peaks one can see that no strong modal frequencies were found. This is due to the strong damping inside the plate. When waves are induced at one end of the plate they have almost vanished when they reach the other end of the plate. On the other hand, reflections can be found when the ball is near the edge of the plate, which will play an important role in the remainder of this paper. (see section 4).

Another important aspect relates to the kind of waves playing a role in the rolling ball system. When a plate is hit by another object, vibrational waves spread from the point of contact over the plate. Following classical plate theory, the vibrational waves are bending waves which are described by a fourth order differential equation. In this case velocity is not independent of frequency but is proportional to the square root of the frequency.

4. Reflections

In a string or membrane the theoretical description of reflections at an open end is relatively straightforward.

Some analytically calculated examples of the reflections for bending waves in bars and for waves reflecting at the surface of a semi-infinite medium indicate, however, that the analysis of the reflections at the free end of a plate is more complicated and that not all energy returns in the reflected waves (see [9]). Instead of deriving the behaviour of the reflections mathematically, their properties will be determined by calculating the correlation function from measured data, in a similar way as treated by Bendat and Piersol [11].

In two-dimensional structures with reflecting edges, there are many different paths consisting of straight lines running from the excursion point to the measuring point: direct and via one or more edges. When trying to measure these reflections with the auto-correlation function, the peak at $\tau = 0$ was found to be very strong while others were much weaker and difficult to detect precisely. This could be attributed to the dispersion and damping of the waves as they travel across the plate. This was partly solved by using two measuring points instead of one and determining the cross-correlation function between the signals measured at these points (see Figure 3). This correlation procedure was repeated for various bandpass-filtered versions of the signals, which also increased the sharpness of the figures. For two accelerometer signals $f(t)$ and $g(t)$, the cross-correlation function is defined as

$$R_{fg}(\tau) = \lim_{T \to \infty} \frac{1}{2T} \int_{-T}^{T} f(t)g(t-\tau)\mathrm{d}t. \qquad (1)$$

Consider a semi-infinite plate with a single edge as shown in Figure 3. Positioned on the plate are the two accelerometers and a ball impacting the plate. For each accelerometer there are two paths running from the ball to the accelerometers: one direct path from the excitation point; the other reaching the accelerometer after being reflected at the edge. This second path can be modelled as coming from a virtual mirror image at the other side of the edge.

The direct wave $f_0(t)$ arrives first, followed by the reflection from the mirror image. Due to the spreading of the wavefront over a larger region there is a reduction in amplitude given by α_1 and α_2,

$$f(t) = \alpha_1 f_0(t - \tau_1) + \alpha_2 f_0(t - \tau_2), \qquad (2a)$$
$$g(t) = \alpha_3 f_0(t - \tau_3) + \alpha_4 f_0(t - \tau_4). \qquad (2b)$$

Using Equation 1, this cross-correlation function splits up into the weighted sum of four of the original auto-correlation function shifted in time. These auto-correlation functions have peaks at $\tau_3 - \tau_1$, $\tau_3 - \tau_2$, $\tau_4 - \tau_1$ and $\tau_4 - \tau_2$, respectively. If these peaks are spaced widely enough, they can be distinguished separately in the cross-correlation function. As more edges are added, the number of mirror images increases accordingly. For an actual plate with four edges, four mirror images will be found. But these are only mirror images of the first order, representing waves reflected at one edge. Similarly, waves reflected more than once can be considered as coming from mirror images of higher order, resulting in a cross-correlation

function consisting of the weighted sum of a large number of time-shifted auto-correlation functions. As in the MDF plates we used the damping was quite high, the weight factors $\alpha_i \alpha_j$ decreased rapidly with increasing path length. Hence, we will only consider the first-order reflections.

So far, only a fixed excitation point was considered. To obtain useful information about the rolling ball this must be extended to a moving excitation point. In order to study the signal at time t_0, a short segment is gated out by multiplying the signal by a window function $w(t)$ shifted t_0 in time. In each windowed segment, the excitation point, or ball position, is considered fixed. For each t_0, we then calculate the cross-correlation function of this windowed segment, or, expressed mathematically,

$$\mathrm{R}_{fg}(\tau, t_0) = \frac{1}{E_w} \int_{-\infty}^{\infty} f(t)g(t-\tau)w(t-t_0)^2 \mathrm{d}t. \quad (3)$$

A non-overlapping square window function was used with a length of 4.167 ms. In the range of the measured velocities, this corresponds to rolling over a distance of between 2.5 and 6.25 mm. E_w represents the energy of the signal within this window.

It appeared that during rolling the energy of the signal was very unevenly distributed over time, so that one windowed segment could contain a lot more energy than the next. In order to compensate for this, the cross-correlation functions were normalised for energy. We will indicate the so obtained figures with *running cross-correlogram*.

The two-dimensional function given by Equation 3 was then plotted with t_0 on the horizontal axis, and τ on the vertical axis. Hence, for each t_0 considered, the cross-correlation functions were displayed vertically. Their values were converted into a gray scale with higher values being lighter than lower values. An example is presented in the lower panel of Figure 4

When the ball moves over a certain distance, the mirror images move along over the same distance. Depending on the configuration, this can lead to changing differences in path lengths between the excitation point and its images, and the accelerometers. This will result in changes in the position of the peaks in the cross-correlation functions. On the other hand, the position of the ball, its mirror images and the accelerometers are known. Hence, the actual differences in path lengths can be measured. And if, for the moment, it is assumed that the wave velocity is constant, and the time differences with which the waves travel these distances can be compared with the positions of the peaks in the measured cross-correlation functions. This provides us with a way to verify whether or not, in the complicated situation of a real plate with its dispersion and its damping, these reflections are very different from the simplified theoretical cases.

In the upper panel of Figure 4 we plotted the calculated maxima of the running cross-correlogram under the assumption that the waves travel with a velocity of 300 m/s. These lines are only plotted if the travelling distance from the origin, and hence the attenuation of the signal, is less
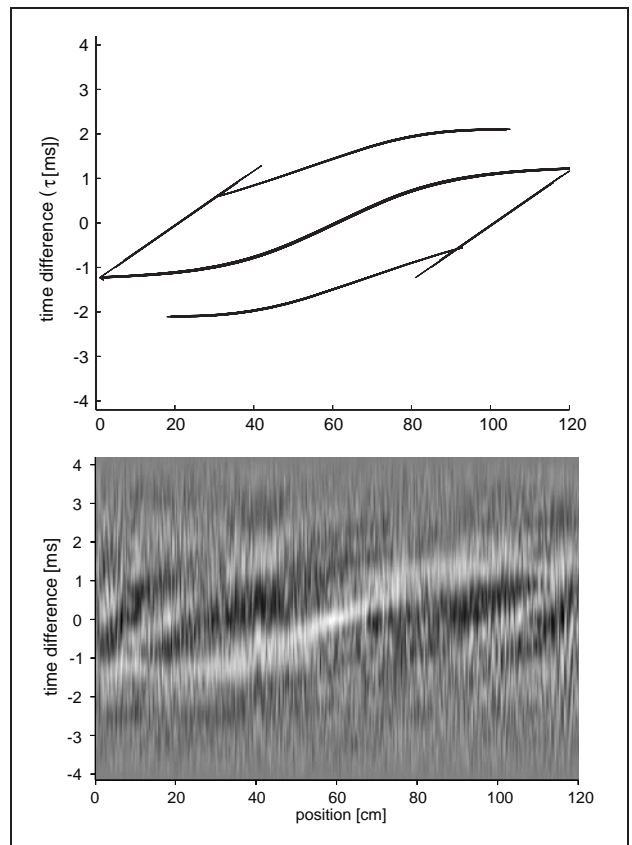

Figure 4. The pattern in the running cross-correlogram, as calculated (above) and measured (below). The two accelerometers were mounted at the edge of the plate on $1/3$ and $2/3$ of its length. The calculated lines approximate the measured ones.

than some specified value. Energy loss at the reflections was not taken into account.

The lower panel displays the actually measured running cross-correlogram. If the position of the lines in the upper panel is compared with the light bands representing the maxima in this running cross-correlogram, the correspondence is indeed remarkable.

Note that in this simplified description it is assumed that the waveform is not distorted too much in the course of travelling through the plate. This implies that the wave velocity is more or less constant, and that issues like dispersion and energy loss at the edges have not yet expressed themselves in clear changes in shape of the wavefront. The correspondence between the two patterns described in the lower and upper panel of Figure 4 shows that, to a certain extent, this is indeed fulfilled. This can partially be explained by the limited frequency range of the excitation. So it can be concluded that the reflected waves are strongly correlated with the original waves. It will be shown later that the resulting similarities between original and reflected waves are the origin of the interference pattern as found in the spectrogram of the rolling sounds.

5. Wave velocity

In the previous sections the wave velocity was regarded as constant. To calculate maxima in the patterns seen in the running cross-correlogram, we had to estimate the wave velocity. Now things can be turned around. One may try to estimate the wave velocity from the running cross-correlogram. This can be done by calculating, for a plausible range of velocities, the correspondence of the calculated lines of maxima with the actual maxima in the measured running cross-correlogram. This has been done informally by printing the calculated lines on top of the measured running cross-correlograms, or by summing, for the range of velocities considered, the values of the running cross-correlogram underneath the calculated lines. The highest value is then expected to represent the best estimate of the wave velocity. This procedure still assumes that the wave velocity is constant within the frequency band of the acoustic signal, and it was shown that possible discrepancies did not distort the reflected signal too much. Classical plate theory predicts, however, that the travelling-wave velocity is proportional to $\sqrt{\omega}$.

Dispersion of the waves leads to a change in shape of the reflected wave, and thus the correlation technique will have to be adapted. In practise the correlation function is blurred due to this dispersion, which means that in stead of well defined narrow and high peaks, smooth broader and lower ones will be found. The amount of blurring depends on the range of frequencies in the waves and the distance they have travelled.

In order to get a frequency dependent estimate of the wave velocity, we will now carry out the above mentioned procedure for a series of band-pass filtered signals. The centre frequencies of the filters ranged from 1 to 10 kHz. Indeed, Figure 5 shows two running cross-correlograms, one for a centre frequency of 774 Hz and one for 5995 Hz. As mentioned, we then calculated, for a range of velocities, the fit of the maxima predicted for these velocities with the actual maxima in the running cross-correlograms.

For low frequencies, the wavelength is no longer small compared to the travelling distances, and this method loses its accuracy. The measured values are plotted in figure 6 from 1 kHz (wavelength about 25 cm) to 10 kHz.

To verify the plausibility of these values, the Young's modulus and density of the MDF were measured. The Young's modulus was measured by statically loading a strip cut from the plate with various weights, in the same direction as the plate is distorted by bending waves. This is the direction in which the wood particles are pressed together, and Young's modulus measured in this way (5.7 kN/mm^2) is somewhat higher than the (true) Young's modulus, measured in other directions (4.2 kN/mm^2). From these measurements the theoretical wave velocity can be calculated. The phase velocity is also measured by determining the frequency of the first resonance mode of a smaller plate. This smaller plate, as well as the strips used for the measurements of the Young's modulus where sawn off the plates used to generate the rolling sounds before the
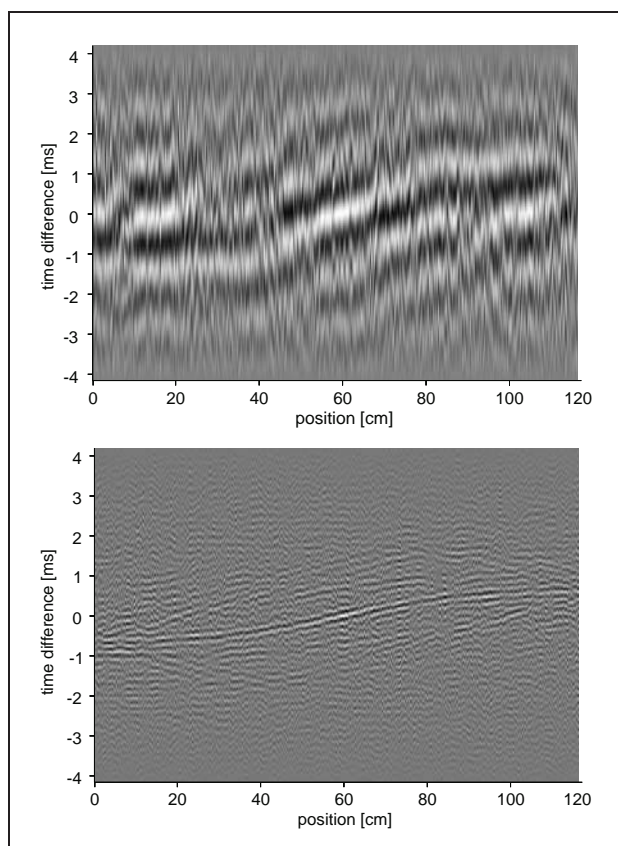

Figure 5. The running cross-correlograms of signals that were first filtered with a bandpass filter. The centre frequency of the filter was 774 Hz for the upper panel and 5996 Hz for the lower panel. The pattern is compressed in the y-direction in the case of the highest band-filter, due to the higher wave velocity for higher frequencies.
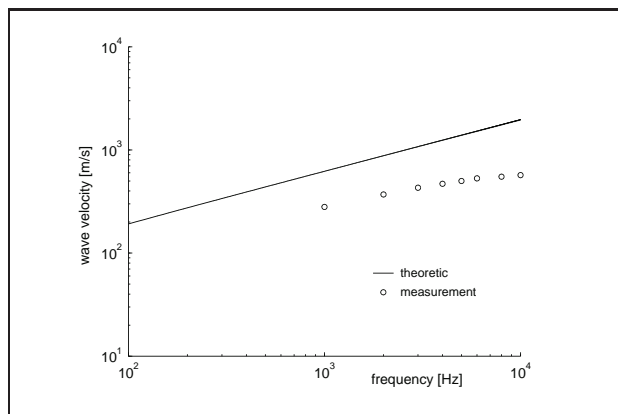

Figure 6. The bending-wave velocity can be estimated by matching measured data with analytically calculated lines of the filtered running cross-correlogram. These estimated values are indicated here with a circle. The line indicates the theoretical group velocity obtained using the theoretical wave velocity, from the statically measured Young's modules.

experiments. The resulting wave velocity at the first mode of this smaller plate (52 Hz) is 50 m/s, quite close to the theoretical value based on the statically measured Young's modulus (56 m/s).

In Figure 6 the group velocity, as calculated via the statically measured Young's modulus is compared with those measured via the correlation method, described above. As can be seen, there appears to be a systematic error increasing with frequency, resulting in measured velocities that are about half as high as the theoretical values based on the statically measured Young's modules. This could be caused by, for instance, internal friction or dispersion, two aspects that are not included in the model.

The velocity found when we do not filter the signal before determining the cross correlate (see Figure 4) is indeed about equal to the velocity of strongest frequencies (see Figures 2 and 6).

6. Comb-filter model for reflections at the edge

In the previous section it was shown that, in our configuration of a metal ball on an MDF plate, the waves, generated at the point of contact between ball and plate, travel through the plate obeying classical plate theory. Moreover, these waves reflect at the edges of the plate and interfere with the direct, unreflected waves. Damping and dispersion are, on the one hand, so high that reflections of higher order do not play a role of significance. On the other hand, the distortion is not so strong that the similarity between direct and reflected waves is lost.

The presence of reflections can be described on the basis of virtual sound sources, so-called mirror images as already depicted and described (see Figure 3). Let us for the moment consider only two mirror images moving in directions opposite to the original ball as shown in Figure 7. One mirror image is positioned at the other side of the edge the real ball leaves behind, while the second mirror image approaches the real ball from the other side of the edge that the ball rolls to. This can be modelled as shown in Figure 8. The delay between direct waves and reflected waves can be calculated by:

$$\tau_1(t) = l/c = (vt)/c, \tag{4a}$$
$$\tau_2(t) = (L - vt)/c, \tag{4b}$$

where c is the group velocity of the vibrational waves in the plate, v the velocity of the ball and l is the distance from the mirror image to the real plate. The attenuation factors α are also time dependent. They decrease for mirror images moving away from the real ball and increase for mirror images approaching the ball. If dispersion and damping are neglected, they can be approximated by

$$\alpha_1(t) = \alpha_0 l = \alpha_0 vt, \tag{5a}$$
$$\alpha_2(t) = \alpha_0(L - vt). \tag{5b}$$

In the configuration we used, it appeared that the damping was so large that the α's almost vanished in the middle of the plane. As a consequence, the model can be simplified by only considering one boundary at a time.
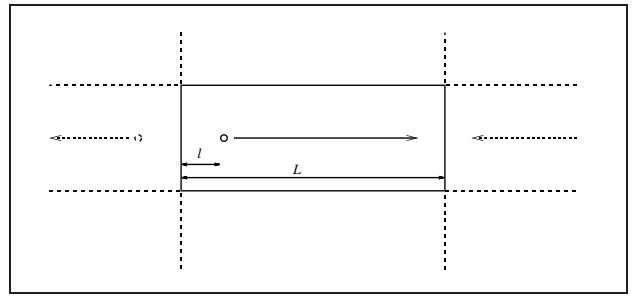

Figure 7. The position of the two most important mirror images considered in the comb-filter model. Indicated are the directions in which the ball and its images rolls, as well as the distances, l and L, used in the formula's.
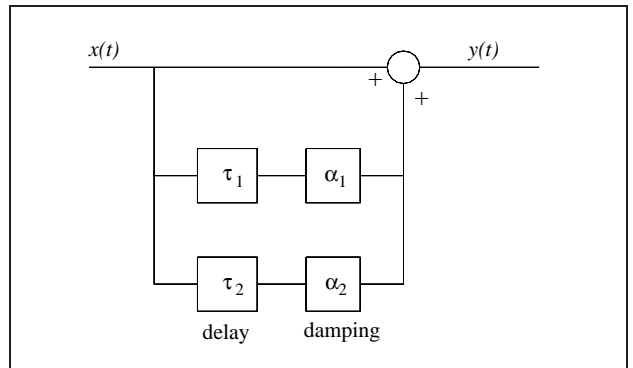

Figure 8. Model for the effect of the images. The two delayed and damped versions of the direct waves are added to this direct wave, due to the effect of reflecting at the boundaries of the plate.

Let us now look at the consequences of the reflections on the spectrum of the rolling sound. The complex spectrum of the direct sound will be indicated with $X(\omega)$; the direct sound plus the reflected sound will be indicated with $Y(\omega)$. If just one reflection is considered, as argued in the previous paragraph,

$$Y(\omega) = X(\omega) + \alpha_i e^{-j\omega\tau_i} X(\omega), \tag{6}$$

then the transfer function $H(\omega)$ and its power spectrum $|H(\omega)|^2$ can be calculated as

$$|H(\omega)|^2 = 1 + \alpha_i^2 + 2\alpha_i \cos(\omega\tau_i) \tag{7}$$

with $i = 1$ or 2 for the desired edge.

This shows that the power spectrum of the combined sound can be calculated from the spectrum of the direct sound by multiplying the spectrum of the direct sound by a constant plus a cosine. This results in a rippled spectrum. Using Equation 4 and 7, it can be shown that the minima of this ripple are located at

$$\omega = \frac{(2n + 1)\pi c}{l}, \tag{8a}$$
$$\omega = \frac{(2n + 1)\pi c}{L - l}, \tag{8b}$$

with $n = 0, 1..\infty$.

The power spectrum for one fixed, frequency-independent τ is plotted as the dashed line in Figure 9. As a consequence of the frequency dependence of the wave velocity, $c = \sqrt{\omega}c'$, the time delay τ_i in between the arrival of the direct and reflected wave is not a constant value but frequency dependent

$$\tau_i = \frac{\tau_i'}{\sqrt{\omega}}, \tag{9}$$

resulting in the power spectrum

$$|H(\omega)|^2 = 1 + \alpha_i^2 + 2\alpha\cos(\sqrt{\omega}\tau_i'), \tag{10}$$

and now the minima of this ripple are located at

$$\omega = \left(\frac{(2n+1)\pi c'}{l}\right)^2, \tag{11a}$$

$$\omega = \left(\frac{(2n+1)\pi c'}{L-l}\right)^2. \tag{11b}$$

The pattern of the minima in the power spectrum can be scaled in two ways. First, increasing the size L of the plate results in a wider pattern. Second, varying c/l, for instance, by varying the thickness of the plate, changes the steepness of the patterns. Note that the patterns do not depend on the ball velocity but on the ball position.

This final result is compared with measurements in Figure 10, where the minima are depicted with lines in the upper panel and are seen as strokes of a lighter colour in the lower panel. Due to the earlier mentioned effects as dispersion and damping, the waves are not completely cancelled at the minimum, which would result in completely white strokes.

7. Synthesis

Next, we tried to get an impression of the perceptual effect of this rippled spectrum, by simulating the effect on synthesised noise and comparing it with the original noise. The synthesis algorithm was divided in two steps. We have started from Gaussian white noise and filtered it in such a way that its long-term power spectrum matched the average power spectrum of recorded rolling sound. By doing so, it is assured that all the spectral properties due to ball and plate properties as well as the velocity of the ball, are well represented in the obtained sound. Also spectral effects which are constant in the course of rolling, for instance due to the radiation from the plate, are taken into account by this step. All temporal properties, however, are ignored by this procedure. Hence, the direct signal consists of band-pass filtered noise. The noise coming from the mirror images can then be added to the original noise according to the attenuated delay modelled in Figure 8. This was first simulated for a frequency independent wave velocity. In this case the result appeared to sound somewhat overdone. This is a consequence of a very prominent so-called repetition pitch in this simulation. The perceptual background of repetition pitch will be described be-
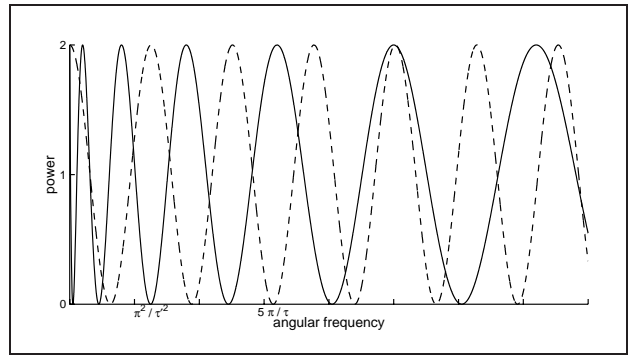

Figure 9. Power spectrum of the model for the effect of the images, here drawn for $\alpha = 1$ and a fixed wave velocity (dashed line) or a frequency dependant wave velocity (solid line). The minima depend on τ, and τ itself depends upon the ball position.
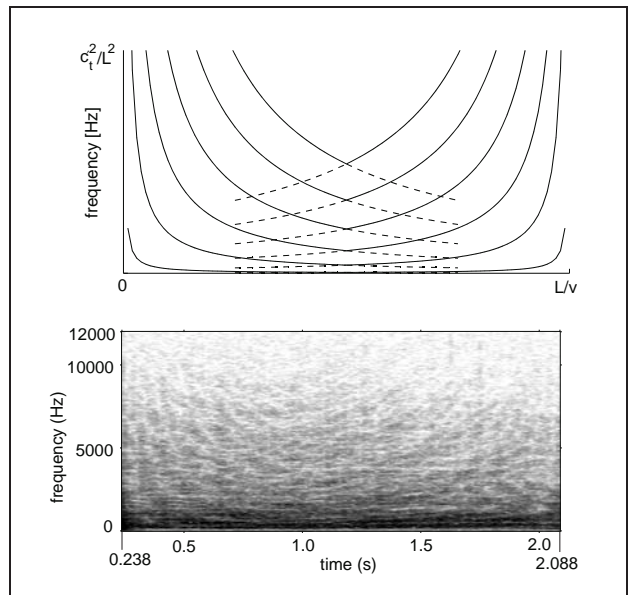

Figure 10. In the spectrogram of a ball rolling from one side to another over an approximately free plate, U-shaped strokes of a lighter colour appear, indicating less power at these frequencies. These are drawn schematically in the upper panel and calculated from measurements in the lower panel.

low. Adding more mirror images in the simulation did not result in any further improvement in the naturalness of the simulated rolling noise. A considerable improvement was obtained, however, when the simulation included that the wave velocity is frequency-dependant. The perceptual effect of the too prominent repetition pitch disappears. The effect of the spectro-temporal pattern is still well audible, and results in a considerable improvement of the naturalness of the sound.

8. Repetition pitch of echoed noise

The study of repetition pitch has been of great interest to pitch-perception research. Repetition pitch can be perceived when a signal, generally a noise signal, is delayed and added to itself. The frequency of the pitch perceived

corresponds to the inverse of the time delay between the two signals. Yost and Hill [12] use a model, similar to the one shown in Figure 8, to generate these repeated-noise signals. They concluded that a pitch can be detected even if one signal is up to 20dB weaker than the other, or, applied to our situation, the reflection can be up to 20 dB weaker than the direct signal. Some signal alterations have been applied to the delayed signal such as filtering (Yost [13]) or phase shift (Bilsen [14]), and this is shown not to influence the presence of a repetition pitch. However, the perceived prominence of the pitch may decrease with these alterations of the signal.

In our situation of the ball rolling over the plate there are some differences with the repeated noise used above. First, the delay between the two noise sources varies with time. If the wave velocity would be independent of frequency, this would result in a time-varying repetition pitch. When the frequency dependence of the wave velocity is taken into account, the situation is more complex. In that case, the ripple on the power spectrum is no longer strictly periodic (see continuous line in Figure 9). Hence, a well defined repetition pitch can no longer be perceived. Rather, the non-periodic ripple colours the spectrum in a more indefinite way. When the ball approaches the edge which reflects the waves, the ripples on the spectrum become more widely spaced. Subjectively, one can hear that something gets higher. But since the ripple on the spectrum in not periodic, this, now, is not perceived as a strict increase in pitch. Neither is it perceived as a change in brightness or sharpness, as these measures are defined as the balance between high and low frequencies, which remains constant in our case (for a definition of the various sound qualities see [15][16]). Furthermore this effect becomes stronger when the ball comes closer to the edge, because the reflections are strongest there.

Note that the interference pattern consists of a change in time of a non-periodic ripple over the spectrum. Integration, either in the time or in the spectral domain results in obscuring or vanishing of this interference pattern. Hence, if human listeners indeed extract information from this interference pattern as to the position and the velocity of the rolling ball, this information resides essentially in the spectro-temporal domain.

9. Discussion

In our study of the sound of a metal ball rolling over a wooden plate, we encountered a spectro-temporal pattern consisting of a time-varying spectral ripple. The spacing of the ripples was not equidistant and decreased with distance from the edge of the plate. By predicting and measuring the running cross-correlogram between two accelerometer signals, it was shown that this pattern was due to the interference between the direct waves generated at the point of contact between ball and plate, and the waves reflected at the edge of the plate. Due to the strong damping in the plate, only first-order reflections had to be taken into account. Higher-order reflections only played a minor role.

In addition, by calculating the running cross-correlograms for different frequency bands, it was shown that the travelling wave velocity was not independent of frequency. In accordance with traditional plate theory the travelling wave velocity increases with the square root of frequency. On the basis of this result, the spectro-temporal interference pattern could quantitatively be described.

It was argued on the basis of the results of pitch-perception research that the human listener is very sensitive to the kind of information present in this spectro-temporal interference pattern. The acoustic vibrations induced by a ball rolling over a wooden plate contain a spectro-temporal pattern listeners can use in estimating the time needed for the ball to reach an edge of the plate. Research by Cabe and Pittenger [17] and Lee and Reddish [18] shows that such information can indeed be gathered from similar properties of the visual or auditory signal. Using this information together with other sources of acoustic information, such as the spectral centroid [5], the spectral tilt, and the temporal variations correlated with the angular speed of the ball (Houben & Stoelinga, [19]), allows the listener not only to estimate physical properties of the ball such as its velocity and its size, but also plate properties such as its material and its dimensions, which can never be perceived on the basis of one parameter alone.

In a following set of perception experiments we will investigate if the information conveyed by this spectro-temporal interference pattern is actually used by human listeners to determine properties such as the ball velocity or the time to reach the edge of the plate. We will do this on the basis of sounds synthesized by simulating the process of direct sound reflected at the edges of a plate. By varying this pattern independent of other physical parameters, which in the natural situation are necessarily coupled and thus correlated with this pattern, we will determine whether indeed the information present in this pattern is used by human listeners in reconstructing an auditory image of what happens around them.

In summary, if accelerometers placed on a wooden plate record the vibrations induced by a metal ball rolling over this plate, the running cross-correlogram of the recorded signals indicate the occurrence of reflections of the waves at the edges of the plate. These running cross-correlograms additionally allow the measurement of the frequency dependent wave velocity in the plate. Moreover, the interference between the direct waves coming from the point of contact between the ball and plate and the waves reflected at the boundary cause a frequency-dependent ripple over the spectrum of the signal. Since the spacing of the ripple becomes wider as the ball approaches the boundary of the plate, the spectrogram shows a time-varying interference pattern. This effect can be described quantitatively by modelling the reflections as coming from mirror images outside the plate. This interference phenomenon is expected to be a source of information the listener uses to estimate the position and the velocity of the rolling ball. Including this interference effect in the synthesis of rolling-ball sounds on the basis of such a simple model in-

deed improves the perceived naturalness of the sound. Especially the frequency-dependence of the wave velocity in the model contributes to this naturalness. As this frequency dependent velocity depends on plate properties such as its material and thickness, this interference pattern may additionally provide the listener with perceptual information for these plate properties. Hence, such models provide the basis for further perception research on rolling sounds.

Acknowledgement

References

[1] D. J. Freed: Auditory correlates of perceived mallet hardness for a set of recorded percussive sound events. Journal of the Acoustical Society of America **87** (1990) 311–322.

[2] S. Lakatos, S. McAdams, R. Caussé: The representation of auditory source characteristics: Simple geometric form. Perception & Psychophysics **59** (1997) 1180–1190.

[3] A. J. Kunkler-Peck, M.T.Turvey: Hearing shape. Journal of Experimental Psychology: Human Perception and Performance **26** (2000) 279–294.

[4] K. van den Doel, P. G. Kry, D. K. Pai: Foleyautomatic: Physically-based sound effects for interactive simulation and animation. SIGGRAPH conference proceedings, 2001.

[5] M. M. J. Houben, A. Kohlrausch, D. J. Hermes: Auditory cues determining the perception of the size and speed of rolling balls. Proceedings of the 2001 International Conference on Auditory Display, Helsinki, Finland, 2001.

[6] D. J. Thompson, B. Hemsworth, N. Vincent: Experimental validation of the twins prediction program for rolling noise, Part 1: Description of the model and method. Journal of Sound and Vibration **193** (1996) 123–135.

[7] D. J. Thompson, P. Fodiman, H. Maé: Experimental validation of the twins prediction program for rolling noise, Part 2: Results. Journal of Sound and Vibration **193** (1996) 137–147.

[8] J. Scheuren: Noise control for cars and trains from an engineering perspective. InterNoise conference proceedings, Nice, France, 2000.

[9] K. Graff: Wave motion in elastic solids. Clarendon Press, 1975.

[10] B. Porat: A course in digital signal processing. Wiley, 1997.

[11] J. S. Bendat, A. G. Piersol: Engineering applications of correlation and spectral analyses. Wiley, 1993.

[12] W. A. Yost: Strengh of the pitches associated with ripple noise. Journal of the Acoustical Society of America **64** (1978) 485–492.

[13] W. A. Yost, R. Hill: The dominance region and ripple noise pitch: A test of the peripheral weighting model. Journal of the Acoustical Society of America **72** (1982) 416–425.

[14] F. A. Bilsen: Repetition pitch: Monaural interaction of a sound with the repetition of the same, but phase shifted, sound. Acoustica **17** (1966) 295–300.

[15] B. C. J. Moore: An introduction to the psychology of hearing. Academic Press, 1989.

[16] E. Zwicker, H. Fastl: Psychoacoustics. Springer-Verlag, 1990.

[17] P. A. Cabe, J. B. Pittenger: Human sensitivity to acoustic information from vessel filling. Journal of Experimental Psychology: Human Perception and Performance **26** (2000) 313–324.

[18] D. N. Lee, P. E. Reddish: Plummeting gannets: a paradigm of ecological optics. Nature **293** (1981) 293–294.

[19] M. M. J. Houben, C. N. J. Stoelinga: Some temporal aspects of rolling sounds. Journées Design Sonore 2002, Paris, France, 2002.